CO_2 Extinction Coefficient 1700–3000 Å

D. E. SHEMANSKY

Department of Physics, University of Pittsburgh, Pittsburgh, Pennsylvania 15213

(Received 2 August 1971)

The CO_2 extinction coefficient in the 1700–3000 Å region has been measured using a 2-m spectrometer in conjunction with a multiple-path absorption cell. The results show excellent agreement with other recent observations to a long-wavelength limit of about 1950 Å. At longer wavelengths the present results indicate considerably lower cross sections; the extinction cross section is dominated by Rayleigh scattering in the region longward of 2035 Å, with values determined reasonably accurately by calculations using the measured refractive index and depolarization factor.

I. INTRODUCTION

The extinction coefficient of CO_2 in the region longward of 1650 Å has recently been the subject of enhanced interest possibly due mostly to the importance of this region to the photochemistry of the Martian atmosphere (cf. McElroy and Hunten[1]). However, measurements in this region up to the point where Rayleigh scattering dominates the extinction coefficient have not been particularly well established. The spectral position at which the Rayleigh scattering cross section dominates extinction as well as the magnitude of the scattering cross section have been uncertain; although the refractive index is accurately determined down to 2379 Å (Koch[2]), the depolarization factor is large (Bridge and Buckingham[3]) and there is some uncertainty in its spectral stability.

Measurements in the spectral region of interest have been made by Ogawa,[4] Heimerl,[5] Inn *et al.*,[6] and Thompson *et al.*[7] The measurements in Ref. 4 are the only available values at wavelengths longward of 1970 Å other than those presented here. Measurements in Refs. 4 and 5 (1650–1820 Å) and Ref. 6 ($\lambda<1750$ Å) all appear to be in agreement in the 1700-Å region, but the values in Refs. 4 and 6 at longer wavelengths are generally lower by 40%–50% than those of Refs. 5 and 7 (1860–1970 Å).

Further measurements in the 1700–3000-Å region using a multiple-path absorption cell (cf. Shemansky[8,9]) are presented below. These results are in excellent agreement with the values of Refs. 4 and 6 up to a long-wavelength limit of about 1950 Å. At wavelengths $\lambda>1950$ Å, the present results tend to be lower by as much as a factor of 4 than those of Ref. 4. It is suggested that the measurements in Ref. 4 in this region may be affected by scattered short-wavelength radiation. According to the discussion below, the CO_2 extinction coefficient is determined reasonably accurately by Rayleigh scattering in the $\lambda>2035$-Å region, as calculated with the Ref. 2 refractive index and the depolarization factor measured at 6328 Å.[3]

II. EXPERIMENT

The experimental arrangement has been described in detail in earlier articles (Shemansky[8,9]). Some minor modifications were made to suit this particular experiment. An absorption chamber with a variable path length was placed at the entrance slit of a 2-m McPherson 240 vacuum spectrometer. Two path lengths were used for the present experiment, 4 and 20 m. The chamber was evacuated with a sorption roughing pump, coupled with a 50-liter/sec differential ion pump. The apparatus was outgassed at a temperature of about 90°C for a period of a few weeks, to obtain a pressure in the region of 10^{-7}–10^{-8} torr. The gas sample was Coleman instrument grade supplied by the Matheson Company, purified by multiple sublimation.

Three sources were used in making the measurements. A xenon-filled quartz tube with an LiF window, excited by a 100-W microwave generator, provided a continuum for observations over the 1700–2500-Å region. A high-pressure Xe short arc illuminator (Varian) with a sapphire window served as a high-intensity source in the region longward of 2000 Å, where difficulties were encountered in the measurement of the very small extinction coefficient. An Hg line source was used for measurements at line positions $\lambda>2300$ Å.

The location of the absorption cell at the entrance slit of the spectrometer was not ideal for the quantitative observations of a continuum. However, the use of ratio recording techniques and stable sources allowed reasonably accurate measurements. A large dynamic range was obtained by using pulse-counting techniques in the entire system.

Most of the observations were made with a low effective resolution of $\Delta\lambda\approx4$ Å. High-resolution measurements at $\Delta\lambda=0.038$ Å were made in the 2100–2200-Å region and in the 2500-Å region, in order to determine whether the long-wavelength end of the spectrum contained any measurable line structure. Path lengths for the observations varied between about 2×10^{-2} and 30 m·atm.

III. RESULTS AND DISCUSSION

The extinction coefficient (k_λ) was determined through the relation

$$I_0/I_\lambda=\exp(k_\lambda Nl), \qquad (1)$$

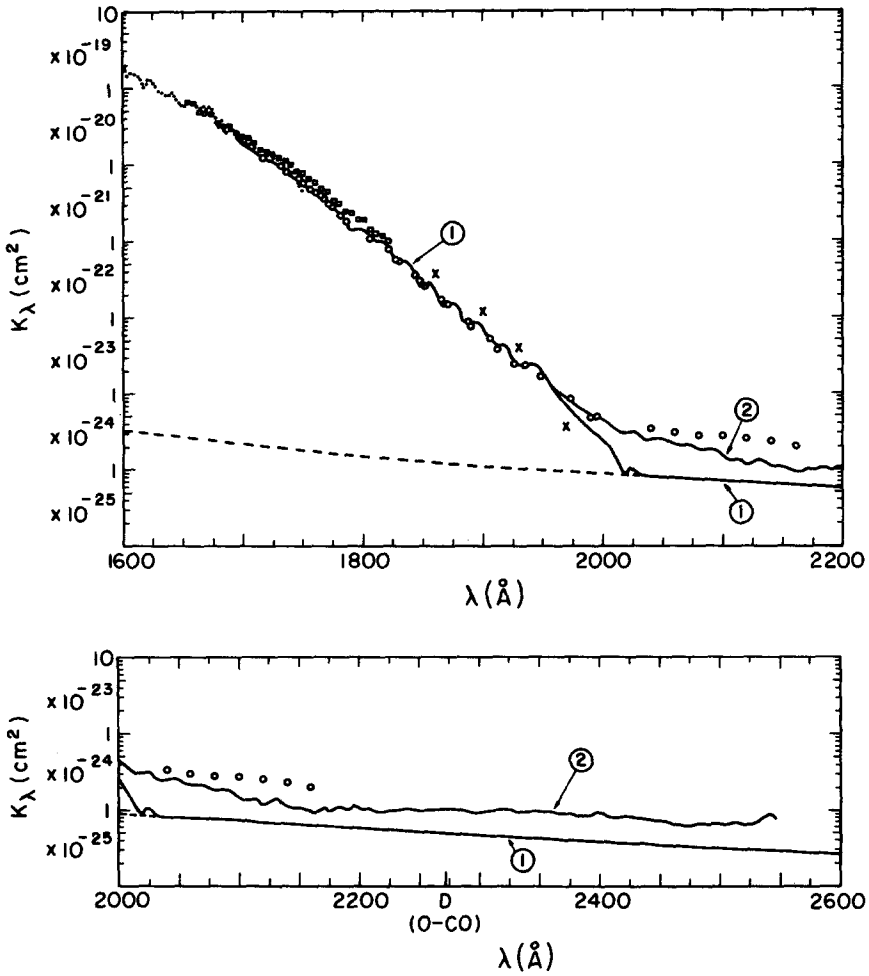

FIG. 1. CO_2 extinction and scattering cross sections 1600–2600 A. —, Present work: curve ①, estimated extinction coefficient; curve ②, measurements with Xe microwave source (see text); - - -, extrapolated Rayleigh scattering cross section (see text); •••, Inn *et al.*[6]; ⊡, Heimerl[5]; ⊙, Ogawa[4]; ×, Thompson *et al.*[7]

where I_0 and I_λ are the transmitted intensities for $N\approx 0$ and $N=N$, respectively, N is the population density of the absorbing molecules, and l is the path length of the incident radiation.

The estimated extinction coefficient (square centimeters) along with earlier estimates, is shown in Table I and Fig. 1. The measurements appeared to be independent of path length, within the accuracy of measurement. The results in the 1695–1800-Å region were obtained with a path length of 1.8×10^{-2} m·atm at a pressure of 3.3 torr. Comparison with the results obtained by Ref. 6 (cf. Ref. 10) show general very good agreement over the entire overlap region, 1695–1750 Å. The measurements in Ref. 6 show structure that is not observed in the present measurements, but this appears to be due to the difference in resolution. Most of the numbers agree to within 10% (cf. Fig. 1). The measurements in the 1800–1885-Å region were obtained with a path length of 0.73 m·atm at a pressure of 27.7 torr. The longer-wavelength measurements were made at path lengths of 21.4 and 29 m·atm. The present results are in very good agreement with those of Ref. 4 over the 1695–1940-Å region, both in absolute value and gross structure (Fig. 1). Deviations from the measurements in Ref. 4 in this region are generally 10% or less. The measurements by Ref. 5 (1655–1825 Å) agree well with these results at 1695 Å, but tend to be higher by about 20%–40% at longer wavelengths. The measurements in Ref. 7 in the 1860–1970-Å region also tend to be larger by factors of 40%–50% in the 1860–1925-Å region, but fall below the present results at 1950 Å. There appears to be no obvious explanation of the discrepancy with Refs. 5 and 7, especially in view of the measurement technique employed by Ref. 5. At wavelengths $\lambda > 1940$ Å, the present results tend to rapidly fall below those of Ref. 4 by factors of 1.5 at 1990 Å and 4 at 2040 Å (Fig. 1). In the author's opinion, this discrepancy in the long-wavelength region may possibly be due to scattered short-wavelength radiation in the case of the measurements of Ref. 4 as a result of the experimental method, in view of similar difficulties encountered in the present work. We discuss the measurements in the region $\lambda > 1950$ Å in some detail, due to the importance of determining the contribution of Rayleigh scattering to the extinction cross section.

TABLE I. CO_2 extinction coefficient 1700–3000 Å.[a]

1695.7	1696.7	1697.7	1698.7	1699.7	1700.8	1701.8
2.47-20	2.43-20	2.35-20	2.23-20	2.07-20	1.95-20	1.90-20
1702.8	1703.8	1704.8	1705.8	1706.8	1707.8	1708.8
1.86-20	1.82-20	1.84-20	1.85-20	1.84-20	1.83-20	1.78-20
1709.9	1710.9	1711.9	1712.9	1713.9	1714.9	1716.0
1.76-20	1.74-20	1.69-20	1.58-20	1.48-20	1.43-20	1.42-20
1717.0	1718.0	1719.0	1720.0	1721.0	1722.0	1723.0
1.39-20	1.31-20	1.23-20	1.21-20	1.24-20	1.26-20	1.24-20
1724.0	1725.1	1726.1	1727.1	1728.1	1729.1	1730.1
1.22-20	1.20-20	1.19-20	1.14-20	1.08-20	1.01-20	9.65-21
1731.1	1732.1	7133.1	1734.1	1735.1	1736.2	1737.2
9.42-21	9.05-21	8.65-21	8.62-21	8.72-21	8.50-21	8.02-21
1738.2	1739.2	1740.2	1741.2	1742.3	1743.3	1744.3
7.57-21	7.40-21	7.53-21	7.68-21	7.72-21	7.62-21	7.19-21
1745.3	1746.3	1747.3	1748.3	1749.3	1750.3	1751.4
6.69-21	6.37-21	6.23-21	6.17-21	6.21-21	6.40-21	6.41-21
1752.4	1753.4	1754.4	1755.4	1756.4	1757.4	1758.4
5.96-21	5.44-21	5.15-21	4.95-21	4.70-21	4.48-21	4.40-21
1759.4	1760.4	1761.5	1762.5	1763.5	1764.5	1765.5
4.39-21	4.55-21	4.61-21	4.50-21	4.33-21	4.03-21	3.68-21
1766.5	1767.6	1768.6	1769.6	1770.6	1771.6	1772.6
3.50-21	3.51-21	3.52-21	3.48-21	3.48-21	3.44-21	3.34-21
1773.6	1774.6	1775.6	1776.7	1777.7	1778.7	1779.7
3.16-21	2.92-21	2.81-21	2.68-21	2.64-21	2.66-21	2.70-21
1780.7	1781.7	1782.7	1783.7	1784.7	1785.7	1786.8
2.82-21	2.85-21	2.75-21	2.46-21	2.05-21	1.78-21	1.68-21
1787.8	1788.8	1789.8	1790.8	1791.8	1792.8	1793.8
1.59-21	1.51-21	1.54-21	1.70-21	1.71-21	1.58-21	1.46-21
1794.9	1795.9	1796.9	1797.9	1798.9	1799.9	1800.9
1.40-21	1.39-21	1.38-21	1.41-21	1.40-21	1.45-21	1.66-21
1802.1	1803.1	1804.1	1805.1	1806.1	1807.1	1808.1
1.59-21	1.58-21	1.50-21	1.37-21	1.23-21	1.11-21	1.05-21
1809.1	1810.1	1811.1	1812.2	1813.2	1814.2	1815.2
1.03-21	1.02-21	1.01-21	1.01-21	1.00-21	9.98-22	9.87-22
1816.2	1817.2	1818.3	1819.3	1820.3	1821.3	1822.3
9.87-22	9.95-22	9.97-22	1.00-21	1.00-21	9.64-22	8.91-22
1823.3	1824.3	1825.3	1826.3	1827.4	1828.4	1829.4
8.21-22	7.70-22	7.29-22	6.82-22	6.22-22	5.66-22	5.29-22
1830.4	1831.4	1832.4	1833.4	1834.4	1835.4	1836.4
5.10-22	5.15-22	5.21-22	5.30-22	5.56-22	5.91-22	6.11-22
1837.4	1838.5	1839.5	1840.5	1841.5	1842.5	1843.6
6.17-22	6.19-22	5.99-22	5.53-22	4.98-22	4.51-22	4.07-22
1844.6	1845.6	1846.6	1847.6	1848.6	1849.6	1850.6
3.72-22	3.48-22	3.29-22	3.14-22	3.04-22	2.91-22	2.86-22
1851.6	1852.7	1853.7	1854.7	1855.7	1856.7	1857.7
2.83-22	2.81-22	2.89-22	3.04-22	3.19-22	3.34-22	3.45-22

TABLE I (*Continued*)

1858.7	1859.7	1860.7	1861.7	1862.7	1863.8	1864.8
3.40-22	3.18-22	2.94-22	2.59-22	2.18-22	1.93-22	1.77-22
1865.8	1866.8	1867.8	1868.8	1869.8	1870.9	1871.9
1.61-22	1.49-22	1.44-22	1.47-22	1.50-22	1.49-22	1.49-22
1872.9	1873.9	1874.9	1875.9	1876.9	1878.0	1879.0
1.50-22	1.50-22	1.50-22	1.65-22	1.81-22	1.83-22	1.79-22
1880.0	1881.0	1882.0	1883.0	1884.0	1885.0	1886.0
1.66-22	1.47-22	1.25-22	1.14-22	1.07-22	8.99-23	8.57-23
1887.0	1888.1	1889.1	1890.1	1891.1	1892.1	1893.1
8.23-23	7.96-23	7.72-23	7.63-23	7.60-23	7.76-23	7.95-23
1894.1	1895.1	1896.1	1897.1	1898.2	1899.2	1900.2
8.10-23	8.20-23	8.35-23	8.59-23	8.77-23	8.67-23	8.23-23
1901.2	1902.2	1903.2	1904.2	1905.2	1906.3	1907.3
7.65-23	7.08-23	6.56-23	6.10-23	5.69-23	5.38-23	5.16-23
1908.3	1909.3	1910.3	1911.3	1912.3	1913.4	1914.4
5.00-23	4.87-23	4.72-23	4.55-23	4.40-23	4.31-23	4.32-23
1915.4	1916.4	1917.4	1918.4	1919.4	1920.4	1921.4
4.40-23	4.49-23	4.52-23	4.51-23	4.51-23	4.49-23	4.34-23
1922.5	1923.5	1924.5	1925.5	1926.5	1927.5	1928.6
4.03-23	3.64-23	3.27-23	2.97-23	2.75-23	2.62-23	2.57-23
1929.6	1930.6	1931.6	1932.6	1933.6	1934.6	1935.6
2.56-23	2.54-23	2.50-23	2.46-23	2.40-23	2.32-23	2.25-23
1936.6	1937.6	1938.7	1939.7	1940.7	1941.7	1942.7
2.22-23	2.24-23	2.31-23	2.38-23	2.40-23	2.38-23	2.33-23
1943.7	1944.7	1945.7	1946.7	1947.7	1948.8	1949.8
2.29-23	2.26-23	2.22-23	2.17-23	2.13-23	2.10-23	2.07-23
1950.8	1951.8	1952.8	1953.8	1954.8	1957.5	1960.0
2.04-23	2.01-23	1.93-23	1.82-23	1.67-23	1.2-23	1.0-23
1962.5	1965.0	1967.5	1970.0	1972.5	1975.0	1977.5
9.0-24	8.2-24	7.4-24	6.6-24	5.9-24	5.4-24	4.9-24
1980.0	1982.5	1985.0	1987.5	1990.0	1992.5	1995.0
4.5-24	4.0-24	3.8-24	3.4-24	3.2-24	3.0-24	2.9-24
1997.5	2000.0	2002.5	2005.0	2007.5	2010.0	2012.5
2.7-24	2.5-24	2.2-24	2.0-24	1.7-24	1.4-24	1.2-24
2015.0	2017.5	2020.0	2022.5	2025.0	2027.5	2030.0
1.0-24	9.0-25	9.0-25	1.0-24	1.0-24	9.5-25	9.0-25
2032.5	2035.0	2037.5	2100.0	2200.0	2380.0	2500.0
8.4-25	8.2-25	8.0-25	7.2-25	5.8-25	4.1-25	3.3-25
2650.0	2750.0	3000.0				
2.5-25	2.1-25	1.46-25				
λ(Å)						
k_λ(cm^2)						

[a] See text.

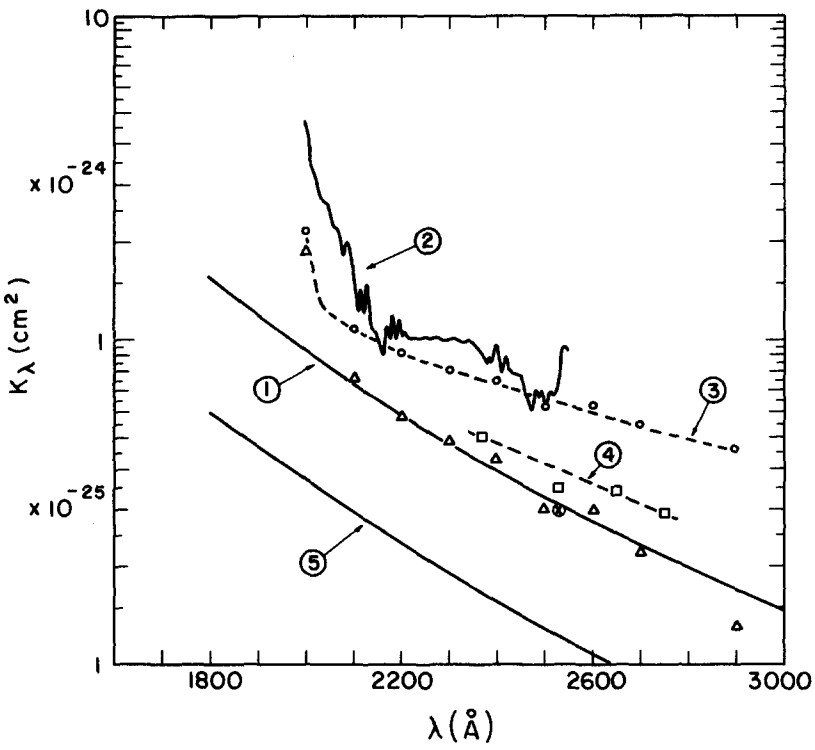

FIG. 2. CO_2 extinction and scattering cross sections 1800–3000 Å. Curve ①, calculated CO_2 Rayleigh scattering cross section (see text); curve ②, present measurements with Xe microwave source; curve ③, present measurements with Xe short arc source; continuous line indicates continuous measurements at resolution $\Delta\lambda = 0.038$ A. Dashed line indicates interpolation between low-resolution measurements at indicated points. Triangled points are the measurements of curve ③ minus 3.3×10^{-25} cm² (see text). Curve ④, best fit line drawn through measurements with Hg line source at the indicated squared points. Curve ⑤, calculated N_2 Rayleigh scattering cross section. Circled cross at 2536 Å indicates measured cross section using Xe short arc source.

Curve ① of Fig. 1 is the present estimated real extinction coefficient. Extinction in the region $\lambda > 2035$ Å is due virtually entirely to Rayleigh scattering, according to these results. Curve ② shows a plot of the measured extinction coefficient using the Xe microwave powered source. The structure on this curve in the long-wavelength region was reproducible and not simply due to measurement noise. The presence of structure beyond the limiting energy for dissociation, $\lambda > 2273$ Å, led to speculation as to whether it originated in gas impurities, scattered short-wavelength emission in the I_0 spectra, or in discrete absorption due to a possible low-lying triplet state of CO_2 (cf. Dixon[11]). Measurements were then made using an Hg line source as a possible measure of the presence of discrete absorption features. These results, at four line positions, were lower by an approximate factor of 2 as shown in Fig. 2 (curve ④). The presence of discrete absorption features was thus considered a distinct possibility at this point in the experimental measurement sequence. Measurements were then made at high resolution, $\Delta\lambda = 0.038$ Å, as mentioned earlier, using a Varian Xe short arc source. The use of this source was considered necessary in order to eliminate possible contributions from scattered short-wavelength radiation and to provide a bright source for high-resolution measurements in the $\lambda > 2000$-Å region. The Xe microwave source was very much brighter at wavelengths $\lambda < 2000$ Å than at longer wavelengths. For this reason the presence of measurable contributions by short-wavelength radiation scattered inside the spectrometer during observations of the I_0 spectrum in the $\lambda > 2000$-Å region, was a distinct possibility; the short arc source produces negligible radiation shortward of 2000 Å. The high-resolution measurements in the 2100–2200- and 2400–2500-Å regions displayed no detectable structure, in sharp contrast to the measurements using the Xe microwave source. Measurements at 100-Å intervals in the 2000–2900-Å region with the short arc source are shown as curve ③ in Fig. 2. Although these measurements fall below curve ②, they remain significantly larger than the Hg line measurements (curve ④). The conclusion then was that the differences between curves ② and ③ were due to scattered short-wavelength radiation in the measurements with the xenon microwave source. The only plausible explanation for the approximately constant difference between curves ③ and ④ appears to arise in the differences in image sizes; the short arc and microwave sources filled the field of view of the absorption cell whereas the Hg line source was much smaller in effective area. This suggests that small changes in image focal position in the region of the spectrometer entrance slit, caused by the introduction of ~1 atm of gas, may account for the disparity with the Hg line measurements. The difference between the measurements of curves ③ and ④ amounts to approximately 2% error in the I_0/I_λ ratio.

Curve ① of Fig. 2 is the Rayleigh scattering cross

section for CO_2 calculated using the relation (Heddle[12])

$$\sigma = (128\pi^5/3\lambda^4)\alpha_0^2[(6+3\rho_n)/(6-7\rho_n)], \quad (2)$$

where σ is the cross section for unpolarized incident radiation, α_0 is the isotropic part of the polarizability, and ρ_n is the normal depolarization ratio. The refractive index for CO_2 has been accurately determined to a lower-wavelength limit of 2379 Å (Ref. 2). However, there is some uncertainty in the calculated Rayleigh scattering cross section, since the depolarization constant is large and has been measured only in the long-wavelength region. The cross section, calculated with the reference 2 refractive index and the value of ρ_n determined from the measurements in Ref. 3 at 6328 Å, is shown as curve 1 of Fig. 2. The depolarization term in Eq. (2) is about 1.14 ($\rho_n = 0.0774$). Curve ① lies approximately constant 0.8×10^{-25} cm^2 below the Hg line measurements and an average of about 3.3×10^{-25} cm^2 below the xenon short arc measurements (curve ③). The triangled points are the short arc measurements after subtraction of 3.3×10^{-25} cm^2 and illustrate the remarkably good conformity to the shape of the Rayleigh scattering curve in the 2100–2900-Å region. It is therefore suggested that the extinction coefficient in the 2100–2900-Å region is due virtually entirely to Rayleigh scattering; at 2000 Å there is an obvious substantial contribution by absorption. In order to confirm the conclusion that the discrepancy in extinction measurement was an artifact of the absorption cell alone, a measurement with N_2 as the scattering gas was made at 2536 Å with the xenon short arc source. Extinction by N_2 is entirely due to Rayleigh scattering in this region, and the cross section is judged to be well determined because of the small depolarization constant.[3,12–15] The measured value was $\sim3\times10^{-25}$ cm^2, compared to the calculated value of 1.2×10^{-25} cm^2 (cf. Fig. 2, curve ⑤). Thus measurements with the absorption cell with ~1 atm of gas tend to place an upper limit on the actual cross section. A lower limit for CO_2 can be obtained by accepting the refractive-index measurements of Ref. 2 and computing Eq. (2) for $\rho_n = 0$. The lower limit estimate at 2500 Å, for example, is then 2.8×10^{-25} cm^2, whereas the upper limit obtained from the measurements with the Hg line source (curve ④) is 4.1×10^{-25} cm^2. It therefore appears that the calculated CO_2 scattering cross section with an assumed constant depolarization factor as measured at 6328 Å (curve ①), is approximately correct with an uncertainty of about the difference between curves ① and ④ (0.8×10^{-25} cm^2). Thus the estimated cross section above ~2040 Å given in the table and by curve ① of Fig. 1 is the calculated Rayleigh scattering cross section.

The estimated cross section in the 1950–2000-Å region has a greater uncertainty than the values in the remainder of the spectrum, since the short arc measurements could not be extended below 2000 Å. However, it was judged that scattered short-wavelength radiation would make a negligible contribution at 1950 Å in the Xe microwave measurements. At 1950 Å, the extinction coefficient was an order of magnitude larger and the relative source intensity was much brighter than the corresponding quantities at 2000 Å. The values between 1950 and 2000 Å are thus a rough interpolation.

Thus according to the interpretation of the measurements presented here, the CO_2 extinction coefficient appears to be fairly well established at wavelengths up to about 1950 Å, although there is no clear reason for the 40%–50% discrepancy with Refs. 5 and 7. The extinction coefficient above 2040 Å appears to be due almost entirely to Rayleigh scattering with some reasonably small uncertainty in the magnitude. Further measurements in this longer-wavelength region would be of interest in view of the disparity between the present measurements and those of Ref. 4.

ACKNOWLEDGMENTS

This work was sponsored by Kitt Peak National Observatory, Tucson, Arizona, operated by the Association of Universities for Research in Astronomy, Incorporated, under contract with the National Science Foundation.

[1] M. B. McElroy and D. M. Hunten, J. Geophys. Res. **75,** 1188 (1970).
[2] J. Koch, Arkiv Mat. Astron. Fysik **10,** No. 1 (1914).
[3] N. J. Bridge and A. D. Buckingham, Proc. Roy. Soc. (London) **295,** 334 (1966).
[4] M. Ogawa, J. Chem. Phys. **54,** 2550 (1971).
[5] J. Heimerl, J. Geophys. Res. **75,** 5574 (1970).
[6] E. C. Y. Inn, K. Watanabe, and M. Zelikoff, J. Chem. Phys. **21,** 1648 (1953).
[7] B. A. Thompson, P. Harteck, and R. R. Reeves, Jr., J. Geophys. Res. **68,** 6431 (1963).
[8] D. E. Shemansky, J. Chem. Phys. **51,** 689 (1969).
[9] D. E. Shemansky, J. Chem. Phys. **51,** 5487 (1969).
[10] J. O. Sullivan and A. C. Holland, GCA Corp. Tech. Rept. #60-20-N, 1964.
[11] R. N. Dixon, Proc. Roy. Soc. (London) **A275,** 431 (1963).
[12] D. W. O. Heddle, J. Quant. Spectry. Radiative Transfer 349 (1962).
[13] D. W. O. Heddle, J. Opt. Soc. Am. **53,** 840 (1963).
[14] J. Koch, Arkiv. Mat. Astron. Fysik **9,** No. 6 (1912).
[15] A. Dalgarno, T. Degges, and D. A. Williams, Proc. Phys. Soc. (London) **92,** 291 (1967).